Am J Cancer Res 2025;15(6):2518-2534
www.ajcr.us /ISSN:2156-6976/ajcr0165419

Original Article

PINX1 inhibits proliferation and cisplatin resistance in nasopharyngeal carcinoma by promoting ILF3 ubiquitination

Ni Zhou[1,2,3*], Pinggui Gong[1,2*], Shuilian Wang[4], Cui He[1,2], Liya Hu[1,2], Hong Peng[1,2]

[1]The Second School of Clinical Medicine, Southern Medical University, Guangzhou 510515, Guangdong, China; [2]Department of Otolaryngology-Head and Neck Surgery, Guangdong Second Provincial General Hospital, Guangzhou 510220, Guangdong, China; [3]Department of Otolaryngology-Head and Neck Surgery, Liuzhou Worker's Hospital, Liuzhou 545007, Guangxi Zhuang Autonomous Region, China; [4]Department of Otolaryngology-Head and Neck Surgery, Foshan Women and Children Hospital, Foshan 528000, Guangdong, China. [*]Co-first authors.

Received April 17, 2025; Accepted May 28, 2025; Epub June 15, 2025; Published June 30, 2025

Abstract: PIN2/TRF1-interacting telomerase inhibitor 1 (PINX1) acts as a tumor suppressor in various cancers, yet its molecular role in nasopharyngeal carcinoma (NPC) remains poorly defined. This study investigates the therapeutic potential of PINX1 in NPC. Expression levels of PINX1 and interleukin enhancer-binding factor 3 (ILF3) were assessed in NPC cells and tissues via western blotting and immunohistochemistry, and their correlation with patient prognosis was analyzed. The effects of ILF3 on NPC cell proliferation and cisplatin resistance were evaluated using cell cycle analysis, EdU incorporation, CCK-8, and IC_{50} assays. Co-immunoprecipitation and immunofluorescence confirmed the interaction between PINX1 and ILF3, while qPCR and western blotting assessed their regulatory relationship. Bioinformatics analysis, chromatin immunoprecipitation, and dual-luciferase assays were performed to identify transcription factors regulating PINX1. Additional in vitro experiments explored the antagonistic relationship between PINX1 and ILF3. Results showed that PINX1 expression was downregulated in NPC and associated with favorable prognosis, whereas ILF3 was upregulated and linked to poor outcomes. PINX1 physically interacted with ILF3 and promoted its ubiquitination through Speckle-type BTB/POZ protein (SPOP). Furthermore, signal transducer and activator of transcription 3 suppressed PINX1 transcription, while PINX1 antagonized the oncogenic effects of ILF3. Mechanistically, PINX1 facilitated ILF3 degradation via SPOP, suppressed the PI3K-AKT-mTOR pathway, inhibited tumor proliferation, and enhanced cisplatin sensitivity in NPC cells. These findings highlight the tumor-suppressive role of PINX1 and underscore its potential as a therapeutic target in NPC.

Keywords: PINX1, ILF3, Nasopharyngeal carcinoma, proliferation, cisplatin resistance, ubiquitination

Introduction

Nasopharyngeal carcinoma (NPC), a malignancy closely linked to Epstein-Barr virus (EBV) infection, shows particularly high incidence rates in southern China and Southeast Asia [1-3]. Radiotherapy, either alone or in combination with chemotherapy, remains the primary treatment for NPC [4]. However, this strategy is often ineffective in advanced-stage disease, where metastasis and resistance to radio- and chemotherapy are the leading causes of mortality. Therefore, there is an urgent need to elucidate the molecular pathogenesis of NPC and identify novel therapeutic targets.

Interleukin enhancer-binding factor 3 (ILF3, also known as NF90/NF110) is a nuclear protein involved in RNA processing and stabilization, and it plays a critical role in cancer cell survival and drug resistance [5]. Elevated ILF3 expression has been linked to enhanced proliferation and chemoresistance in lung adenocarcinoma, possibly through its involvement in anti-apoptotic signaling and stabilization of oncogenic transcripts [6]. Mechanistically, ILF3 encodes a double-stranded RNA-binding protein that forms complexes with proteins, mRNAs, small noncoding RNAs, and dsRNAs, thereby regulating gene expression and maintaining mRNA stability [7-9]. It also modulates

https://doi.org/10.62347/WFER2605

Table 1. Association of ILF3 protein expression with clinical characteristics

Parameters	Case	Low ILF3 expression	High ILF3 expression	χ^2	*P*
Age (n)				0.964	0.326
<50	51	15	36		
≥50	48	10	38		
Sex (n)				0.598	0.439
Male	58	13	45		
Female	41	12	29		
Clinical stages (n)				6.315	0.013
I/II	32	3	29		
III/IV	67	22	45		
T stage (n)				6.528	0.016
T1/T2	37	4	33		
T3/T4	62	21	41		
N stage (n)				7.877	0.005
N0/N1	30	2	28		
N2/N3	69	23	46		
M stage (n)				6.263	0.018
M0	72	23	49		
M1	27	2	25		

Note: χ^2 test was applied to access the correlation between the clinical characteristics and ILF3 expression. T stage: tumor size; N stage: lymph node; M stage: distant metastasis.

transcription, translation, and primary microRNA processing. In the nucleus, ILF3 regulates genes such as TGF-β2 and IL36γ [10, 11]. These functions suggest that targeting ILF3-mediated pathways may offer a promising strategy to enhance NPC therapeutic sensitivity.

PIN2/TRF1-interacting telomerase inhibitor 1 (PINX1) is a well-characterized tumor suppressor that inhibits telomerase activity [12]. Loss of PINX1 is strongly associated with tumorigenesis and progression in various cancers [13-15]. Recent studies indicate that PINX1 also exerts telomerase-independent biological functions [16]. For instance, our previous research found that PINX1 expression is downregulated in NPC, although this downregulation does not appear to be driven by genetic mutations or promoter methylation [17]. Bioinformatics analysis further revealed a potential inverse correlation between PINX1 and ILF3 expression. These findings warrant further investigation into the specific molecular mechanisms by which PINX1 regulates ILF3 in NPC.

Materials and methods

Tissue specimens, cell cultures and animal models

Tissue samples from 131 individuals, including 99 nasopharyngeal carcinoma (NPC) cases and 32 noncancerous nasopharyngeal controls, were collected from Guangdong Second Provincial General Hospital.

Inclusion and exclusion criteria were as follows: (1) pathological diagnosis of NPC confirmed by at least two pathologists; (2) no prior radiotherapy or chemotherapy; (3) absence of other life-threatening diseases; and (4) no malignancies other than NPC. Detailed patient information is presented in **Tables 1** and **2**. All 99 NPC patients subsequently received combined radiotherapy and chemotherapy, with complete five-year follow-up data available.

NPC cell lines were obtained from the Central Laboratory of the Integrated Hospital of Traditional Chinese Medicine, Southern Medical University (Guangzhou, China). NPC cells were cultured in RPMI-1640 medium (Corning) sup-

Table 2. Association of PINX1 protein expression with clinical characteristics

Parameters	Case	Low PINX1 expression	High PINX1 expression	χ^2	*P*
Age (n)				0.210	0.647
<50	51	31	20		
≥50	48	27	21		
Sex (n)				0.700	0.403
Male	58	36	22		
Female	41	22	19		
Clinical stages (n)				5.251	0.022
I/II	32	24	8		
III/IV	67	34	33		
T stage (n)				7.112	0.008
T1/T2	37	28	9		
T3/T4	62	30	32		
N stage (n)				5.800	0.016
N0/N1	30	23	7		
N2/N3	69	35	34		
M stage (n)				5.636	0.018
M0	72	37	35		
M1	27	21	6		

Note: χ^2 test was applied to access the correlation between the clinical characteristics and ILF3 expression. T stage: tumor size; N stage: lymph node; M stage: distant metastasis.

plemented with 10% fetal bovine serum (Corning). The NP69 cell line was cultured in keratinocyte serum-free medium (Gibco, Grand Island, NY, USA) supplemented with recombinant human epidermal growth factor. All cells were maintained at 37°C in a humidified incubator containing 5% CO_2.

This study adhered to the principles of the Declaration of Helsinki. Written informed consent was obtained from all participants. Ethical approval for the use of human tissues and clinical data was granted by the Ethics Committee of Guangdong Second Provincial General Hospital (Approval No. 2021-KZ-160-04).

Female BALB/c nude mice (nu/nu; 4 weeks old, 11-12 g) were purchased from Yoda Biotechnology Co., Ltd. (Guangzhou, China). All animal experiments were conducted in compliance with institutional guidelines and were approved by the Animal Ethics Committee of Guangdong Second Provincial General Hospital (Approval No. 2022-DW-KZ-044-02). Efforts were made to minimize animal suffering and reduce the number of animals used.

siRNA and plasmid transfection

Small interfering RNAs (siRNAs) targeting ILF3, Speckle-type BTB/POZ protein (SPOP), and signal transducer and activator of transcription 3 (STAT3) were designed and synthesized by RiboBio (Guangzhou, China). Plasmids encoding STAT3, PINX1, siPINX1, and ILF3 were obtained from GeneChem (Shanghai, China). NPC cells were seeded into six-well plates at 30-50% confluence and transfected using Lipofectamine 2000 (Invitrogen, Shanghai, China) according to the manufacturer's protocol. Cells were harvested 48-72 hours post-transfection for subsequent experiments.

Lentiviral transduction

Lentiviral vectors carrying short hairpin RNA targeting PINX1 (shPINX1) and corresponding control vectors were constructed by GeneChem (Shanghai, China). Human Nasopharyngeal Epithelial cell line (HONE1 and 5-8F cells) were infected with these lentiviruses. GFP-positive polyclonal cell populations were selected and validated using RT-qPCR and western blotting.

Quantitative PCR (qPCR)

Total RNA was extracted using Trizol reagent (Takara, Shiga, Japan), and cDNA was synthesized using the PrimeScript RT Reagent Kit (Takara, Dalian, China) following the Manufacturer's instructions. qPCR was performed in

triplicate using SYBR Premix Ex Taq (Takara, Dalian, China). Primer sequences were as follows: PINX1: Forward: 5'-CCAGCGGATGCTAGAGAAGAT-3', Reverse: 5'-CGAGTCCCAGGTGGTTATTTTTC-3'; ILF3: Forward: 5'-GAAGACGGAGCACATGACCAGAAC-3', Reverse: 5'-CTTCTCCTTACACAGCAGCACCAG-3'; STAT3: Forward: 5'-GGAGGAGTTGCAGCAAAAG-3', Reverse: 5'-CACACCAGGTCCCAAGAGTT-3'; GAPDH: Forward: 5'-CATGGGTGTGAACCATGAGA-3', Reverse: 5'-GTCTTCTGGGTGGCAGTGAT-3'.

Western blotting

Protein lysates were resolved via SDS-PAGE and transferred to membranes, which were blocked with 5% BSA. Membranes were incubated with the following primary antibodies: STAT3 (1:1000, #9139), p-STAT3 (1:1000, #9145); PI3K (1:1000, #4257), p-PI3K (1:1000, #4228); AKT (1:1000, #9272), p-AKT (1:1000, #4060); mTOR (1:1000, #2792), p-mTOR (1:1000, #2791).

(All Cell Signaling Technology). PINX1 (1:2500, ab190252, Abcam), ILF3 (1:1000, 19887-1-AP), Ubiquitin (1:1000, 10201-2-AP), SPOP (1:1000, 16750-1-AP), CCNE1 (1:1000, 11554-1-AP). (All Proteintech). Flag (1:1000, Sigma), GAPDH (1:1000, CW0100, Cwbio). Protein detection was performed using enhanced chemiluminescence (Millipore, Bedford, MA, USA).

Immunohistochemistry

Paraffin-embedded tissue sections (4 μm) were stained with antibodies against PINX1 (1:200, 12368-1-AP) and ILF3 (1:200, 19887-1-AP) (All Proteintech) using the streptavidin-peroxidase method (ZSGB-BIO, Beijing, China). Two independent pathologists evaluated the slides. Staining scores were calculated based on: (1) the percentage of positive cells (1: <25%, 2: 25-49%, 3: 50-74%, 4: ≥75%), and (2) staining intensity (0: negative, 1: weak, 2: moderate, 3: strong). Total scores were obtained by multiplying the two values. Scores ≤6 were considered low expression; >6 were considered high expression [18].

Cell viability assay

NPC cell viability was measured using the CCK-8 assay (Dojindo, Japan). Cells were seeded in 96-well plates (1,000 cells/well), and after incubation, 10 μL of CCK-8 reagent was added. Absorbance was measured at 450 nm after 2 h incubation at 37°C (time points: Days 1-5).

EdU incorporation and cell cycle assays

DNA synthesis was assessed using an EdU kit (RiboBio, Guangzhou, China) according to the manufacturer's instructions. Fluorescence intensity was quantified using ImageJ software.

For cell cycle analysis, NPC cells were fixed in 70% ethanol at 4°C overnight, treated with RNase A (50 μg/mL) at 37°C, and stained with propidium iodide (50 μg/mL).

Cytotoxicity assay

Cisplatin (DDP, Jinan, China) was dissolved in PBS at a concentration of 0.5 mg/mL. NPC cells were plated in 96-well plates (5×10^3 cells/well) and treated with various DDP concentrations. After 48 h, cell viability was assessed using the CCK-8 assay.

Co-immunoprecipitation (Co-IP) assay

Co-IP was carried out using the Pierce Co-Immunoprecipitation Kit (Thermo Scientific, USA) according to the manufacturer's instructions. Approximately 1,000 μg of total protein was incubated overnight at 4°C with 5 μg of the appropriate antibody or IgG control. Immune complexes were washed, eluted, and analyzed by western blotting.

Immunofluorescence and confocal microscopy

NPC cells were seeded on coverslips in 48-well plates. After cell adherence, the cells were fixed with 4% paraformaldehyde and permeabilized using 0.5% Triton X-100. They were then incubated with primary antibodies against PINX1 (1:100, 12368-1-AP, Proteintech), ILF3 (1:100, 19887-1-AP, Proteintech), and SPOP (1:100, 16750-1-AP, Proteintech). Nuclei were counterstained with DAPI. Imaging was performed using a confocal microscope.

Cycloheximide (CHX) chase assay

NPC cells were transfected with or without PINX1 overexpression and subsequently treated with 50 μg/mL CHX (Abcam, Massachusetts, USA) for 12 h or left untreated. Cells were then

exposed to 20 μmol/L MG132 (Sigma-Aldrich, MO, USA) and protein levels were analyzed by western blotting.

Chromatin immunoprecipitation (ChIP)

Three potential STAT3-binding sites within the PINX1 promoter were identified using the JASPAR database. ChIP was performed in HONE1 and 5-8F cells using the EZ-ChIP Assay Kit (Millipore, Bedford, MA, USA). DNA-protein complexes were immunoprecipitated with either anti-STAT3 antibody (1:50, Cell Signaling Technology) or IgG control. Purified DNA was analyzed by qPCR and agarose gel electrophoresis. Primer sequences were: Site 1 (-1356/1346, motif: CTTTCTGAAAT): Forward: 5'-ACTAACCATTTACCACCTGAACC-3', Reverse: 5'-GCACCTCCTGTGTTGGTATATG-3'; Site 2 (-1327/-1317, motif: GTGCTTGAAAA): Forward: 5'-TGAGTCCAGTGCCCTACTT-3', Reverse: 5'-GGGAGGCAAGTGAATGGAAT-3'; Site 3 (-1139/-1129, motif: TGGCTGGGAAA): Forward: 5'-GCTTCGATCTTCTTGACCATCTT-3', Reverse: 5'-CCAGAGAGAGTGGAAGGTAGTT-3'.

Luciferase reporter assay

DNA fragments containing putative STAT3-binding sites were cloned into the pGL4.1-Basic luciferase reporter vector. Site-specific mutants (MUT1, MUT2, and MUT1+2) were also constructed. Reporter constructs and STAT3 expression plasmids were co-transfected into 293T cells. Luciferase activity was measured 48 hours post-transfection using the Dual-Luciferase Reporter Assay System (Promega, Madison, WI, USA).

Electrophoretic mobility shift assay (EMSA)

EMSA was performed using an EMSA kit (BersinBio, Guangzhou, China) according to the manufacturer's protocol. Nuclear extracts from HONE1 and 5-8F cells were incubated with biotin-labeled oligonucleotide probes targeting the PINX1 promoter. Competition and supershift assays were conducted by adding a 100-fold excess of cold (unlabeled) wild-type or mutant probes or anti-STAT3 antibodies. Signals were detected and analyzed after electrophoresis.

In vivo tumor model

A total of 5×10^6 5-8F cells transduced with either control shRNA (shNC) or shPINX1 were subcutaneously injected into BALB/c nude mice (female, 4 weeks old, 11-12 g). Mice were randomly divided into six groups (n=5 per group) for the following treatments: shNC + saline, shNC + DDP, shPINX1 + saline, shPINX1 + DDP, shPINX1 + DDP + 4 mg/kg Stattic, and shPINX1 + DDP + 2 mg/kg Stattic. Treatments (saline, cisplatin [DDP], or Stattic) were administered intraperitoneally every three days. Tumor growth was monitored, and mice were sacrificed by cervical dislocation 15 days post-inoculation. Tumor nodules were excised, weighed, dried, and processed for paraffin embedding and histological analysis.

Gene set enrichment analysis (GSEA)

Advanced GSEA was performed using the GEO dataset GSE118719.

Statistical analysis

Statistical analyses were performed using GraphPad Prism 10 (GraphPad Software, USA) and SPSS 30.0 (IBM, USA). Data are presented as mean ± standard deviation (SD) from at least three independent experiments. Categorical data were expressed as frequencies (n). Two-group comparisons were assessed using Student's two-tailed t-test. For n<5, apply Fisher's exact test. One-way ANOVA was applied for comparisons among multiple groups and post hoc Bonferroni correction was performed. For repeated measurements across time-points, repeated-measures ANOVA was used. Cox proportional hazards regression was applied to assess independent prognostic variables. Associations between gene expression and clinicopathological parameters were evaluated using chi-square tests (χ^2). Kaplan-Meier survival analysis was used to estimate overall survival, with significance defined as $P<0.05$.

Results

Expression of PINX1 and ILF3 in NPC tissues and cells

Western blotting was used to assess PINX1 and ILF3 protein levels in nasopharyngeal carcinoma (NPC) cell lines (CNE1, CNE2, SUNE1, 5-8F, 6-10B, HONE1, and HONE1-EBV) and in the immortalized nasopharyngeal epithelial cell line NP69. Compared to NP69, PINX1 protein expression was markedly decreased in all NPC

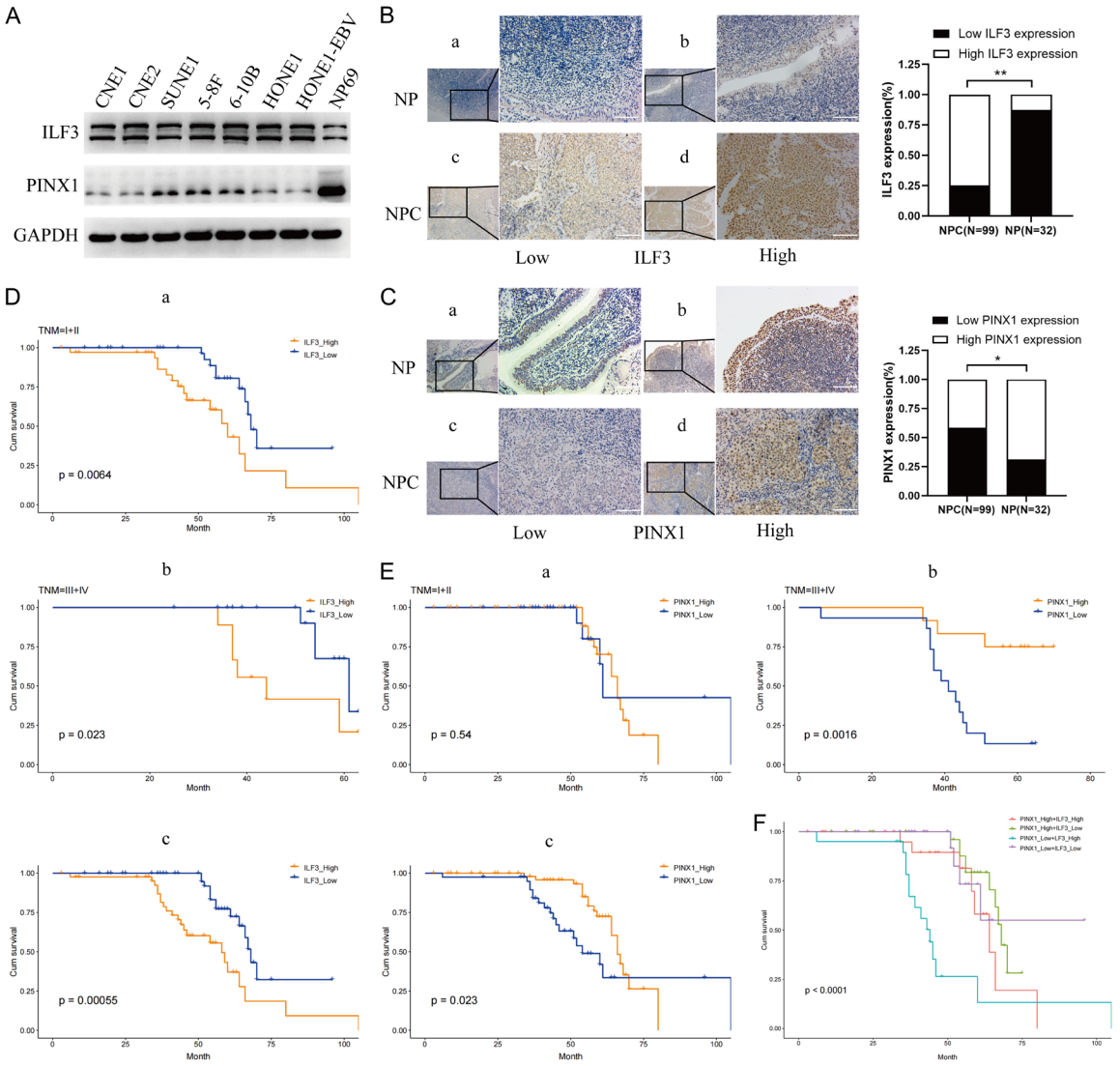

Figure 1. Expression of PINX1 and ILF3 in NPC tissues and cells. Expression of PINX1 is negatively related to that of ILF3 in NPC tissues and cells. A. Western blot assessments of ILF3 and PINX1 levels in NPC cells and NP69 cells; B, C. Immunohistochemistry (IHC) assessments of ILF3 and PINX1 levels in NPC tissues and NP tissues (×200, Scale bar: 100 μm); D-F. Kaplan-Meier survival rate analysis was performed using an in-house cohort collected from Guangdong Second Provincial General Hospital (n=99). ILF3: Interleukin enhancer-binding factor 3; PINX1: PIN2/TRF1-interacting telomerase inhibitor 1; NPC: Nasopharyngeal carcinoma; NP: Nasopharyngeal; *, *P*<0.05; **, *P*<0.01.

cell lines, while ILF3 protein expression was significantly increased (**Figure 1A**).

Immunohistochemical analysis showed that 87.5% (28/32) of noncancerous nasopharyngeal (NP) samples exhibited low ILF3 expression, whereas 74.7% (74/99) of NPC tissues showed high ILF3 expression (**Figure 1B**). Conversely, 68.8% (22/32) of NP tissues displayed high PINX1 expression, while 58.6% (58/99) of NPC samples showed low expression (**Figure 1C**).

Kaplan-Meier survival analysis revealed that, among NPC patients with stage I/II disease, high ILF3 expression was associated with significantly poorer survival than low ILF3 expression. Similar trends were observed in stage III/IV patients and in the overall cohort (**Figure 1D**). In contrast, low PINX1 expression correlated with shorter survival in both early - and late-stage NPC, as well as across the full TNM staging spectrum (**Figure 1E**). Notably, patients with low ILF3 and high PINX1 expression exhibited the most favorable prognosis, whereas

Table 3. Univariate and multivariate Cox regression analysis in 99 NPC patients

Clinical characters	Univariate analysis			Multivariate analysis		
	HR	95% CI	*P*	HR	95% CI	*P*
Age						
<50 vs ≥50	1.005	0.975-1.037	0.732	1.025	0.976-1.075	0.316
Sex						
Male vs female	1.090	0.465-2.553	0.843	0.968	0.378-2.483	0.946
Clinical stages						
I/II vs III/IV	2.119	1.025-4.384	0.043	6.434	2.122-19.531	0.001
T stage						
T1/T2 vs T1/T2	2.989	1.429-6.251	0.004	3.832	1.559-9.419	0.003
N stage						
N0/N1 vs N2/N3	6.402	2.707-15.143	0.004	3.828	1.153-12.715	0.028
M stage						
M0 vs M1	3.576	1.657-7.720	0.001	3.935	1.310-11.814	0.015
ILF3 expression						
Low vs high	3.357	1.563-7.208	0.002	4.845	2.077-11.300	0.000
PINX1 expression						
Low vs high	0.374	0.173-0.805	0.012	0.319	0.127-0.802	0.015

Note: Cox proportional hazard regression model was applied to access the independent prognosticvariables. T stage: tumor size; N stage: lymph node; M stage: distant metastasis; HR: hazard ratio; 95% CI: 95% confidence interval.

those with high ILF3 and low PINX1 had the worst outcomes (**Figure 1F**).

Association between PINX1/ILF3 expression and clinicopathological features

There were no significant differences in age or gender between ILF3 low and high expression groups (both P>0.05). However, ILF3 expression was significantly associated with clinical stage, T stage, N stage, and M stage (all P<0.05; **Table 1**). Similarly, while age and gender showed no significant differences between PINX1 low and high expression groups (all P>0.05), clinical stage, T stage, N stage, and M stage were significantly correlated with PINX1 expression (all P<0.05; **Table 2**). Univariate and multivariate Cox regression analyses in 99 NPC patients indicated that ILF3 and PINX1 expression levels, clinical stage, and TNM classification were independent prognostic factors (**Table 3**).

ILF3 promotes cell proliferation and cisplatin resistance

GSEA analysis suggested that ILF3 may promote cell cycle progression and activate the PI3K-AKT signaling pathway (**Figure 2A**). EdU incorporation, CCK-8, and cell cycle assays confirmed that ILF3 overexpression significantly enhanced NPC cell proliferation, while ILF3 knockdown suppressed proliferation (**Figure 2B-D**).

Cisplatin sensitivity was also affected by ILF3 expression: the IC_{50} of cisplatin in HONE1 cells decreased from 20.32 μM in controls to 10.94 μM in siILF3-transfected cells, and from 21.45 μM to 13.21 μM in 5-8F cells (**Figure 2E**), indicating enhanced sensitivity upon ILF3 knockdown.

Western blotting revealed that ILF3 overexpression increased phosphorylation of PI3K, AKT, and mTOR, without affecting total protein levels. It also upregulated CCNE1 expression. ILF3 knockdown produced the opposite effects (**Figure 2F**).

PINX1 interacts with ILF3

Coomassie brilliant blue staining and mass spectrometry analysis initially suggested an interaction between PINX1 and ILF3 (**Figure 3A**, **3B**). Co-immunoprecipitation assays in HONE1 and 5-8F cells confirmed this interaction (**Figure 3C**). Immunofluorescence further demonstrated nuclear co-localization of PINX1 and ILF3 (**Figure 3D**).

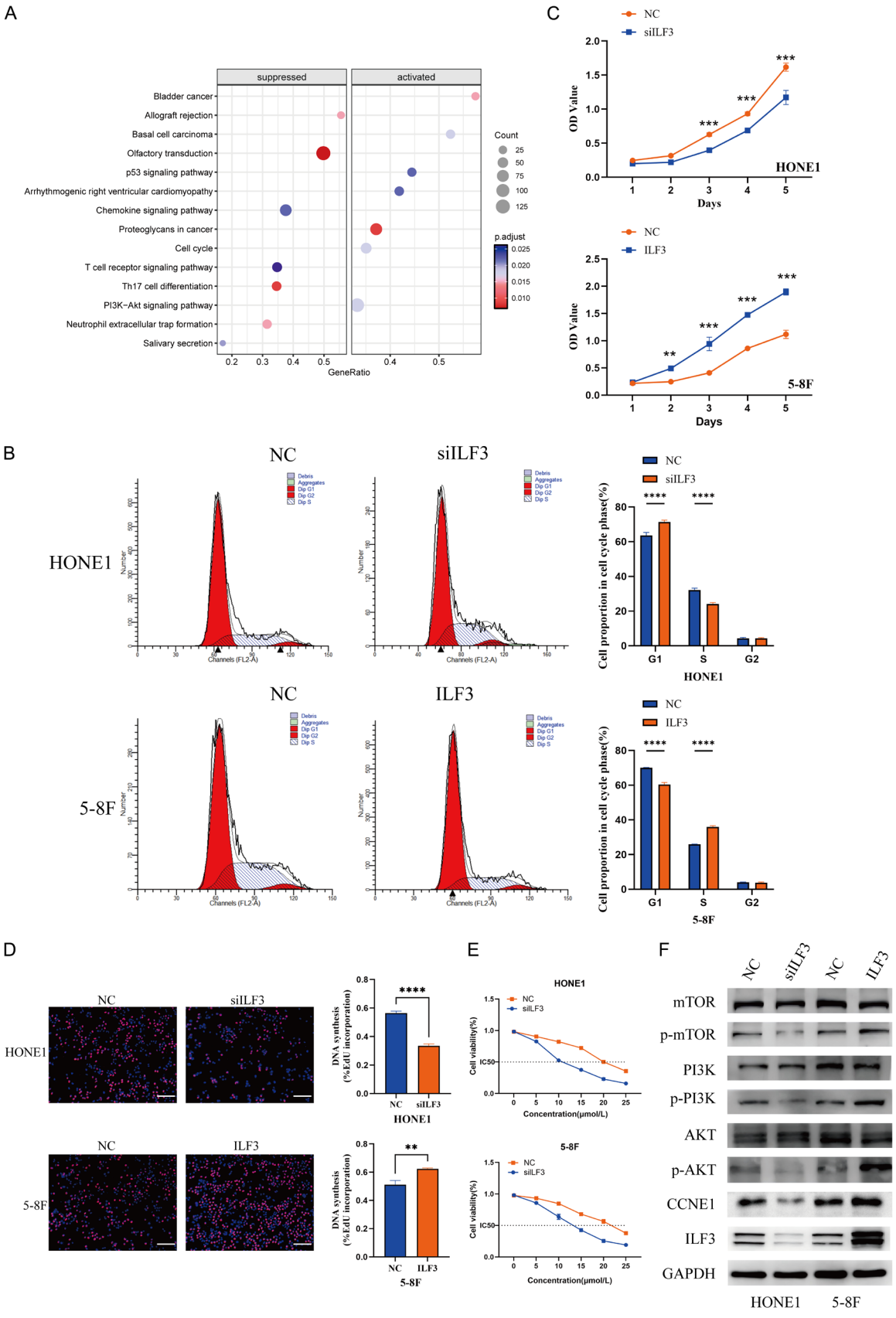
A
suppressed
activated
Bladder cancer
Allograft rejection
Basal cell carcinoma
Olfactory transduction
p53 signaling pathway
Arrhythmogenic right ventricular cardiomyopathy
Chemokine signaling pathway
Proteoglycans in cancer
Cell cycle
T cell receptor signaling pathway
Th17 cell differentiation
PI3K−Akt signaling pathway
Neutrophil extracellular trap formation
Salivary secretion
GeneRatio
Count
p.adjust
C
NC
siILF3
OD Value
Days
HONE1
NC
ILF3
5-8F
B
NC
siILF3
ILF3
HONE1
5-8F
Cell proportion in cell cycle phase(%)
G1
S
G2
D
DNA synthesis (%EdU incorporation)
E
Cell viability(%)
IC50
Concentration(μmol/L)
F
mTOR
p-mTOR
PI3K
p-PI3K
AKT
p-AKT
CCNE1
ILF3
GAPDH

Figure 2. ILF3 promotes cell proliferation and DDP resistance. ILF3 promotes cell proliferation and DDP resistance. A. GSEA analysis indicates how ILF3 is involved in the cell cycle and in activating the PI3K-AKT pathway; B-E. Viability, cell cycle distribution, and half-maximal inhibitory concentration (IC_{50}) of NPC cells DDP were performed using EdU, CCK-8 and flow cytometry assays (×100, Scale bar: 200 μm); F. Western blot analysis of the PI3K-AKT-mTOR signaling pathway using GAPDH as a loading control. ILF3: Interleukin enhancer-binding factor 3; PINX1: PIN2/TRF1-interacting telomerase inhibitor 1; NPC: Nasopharyngeal carcinoma; NP: Nasopharyngeal; HONE1 and 5-8F: Human Nasopharyngeal Epithelial cell line; *, *P*<0.05; **, *P*<0.01; ***, *P*<0.001; ****, *P*<0.0001.

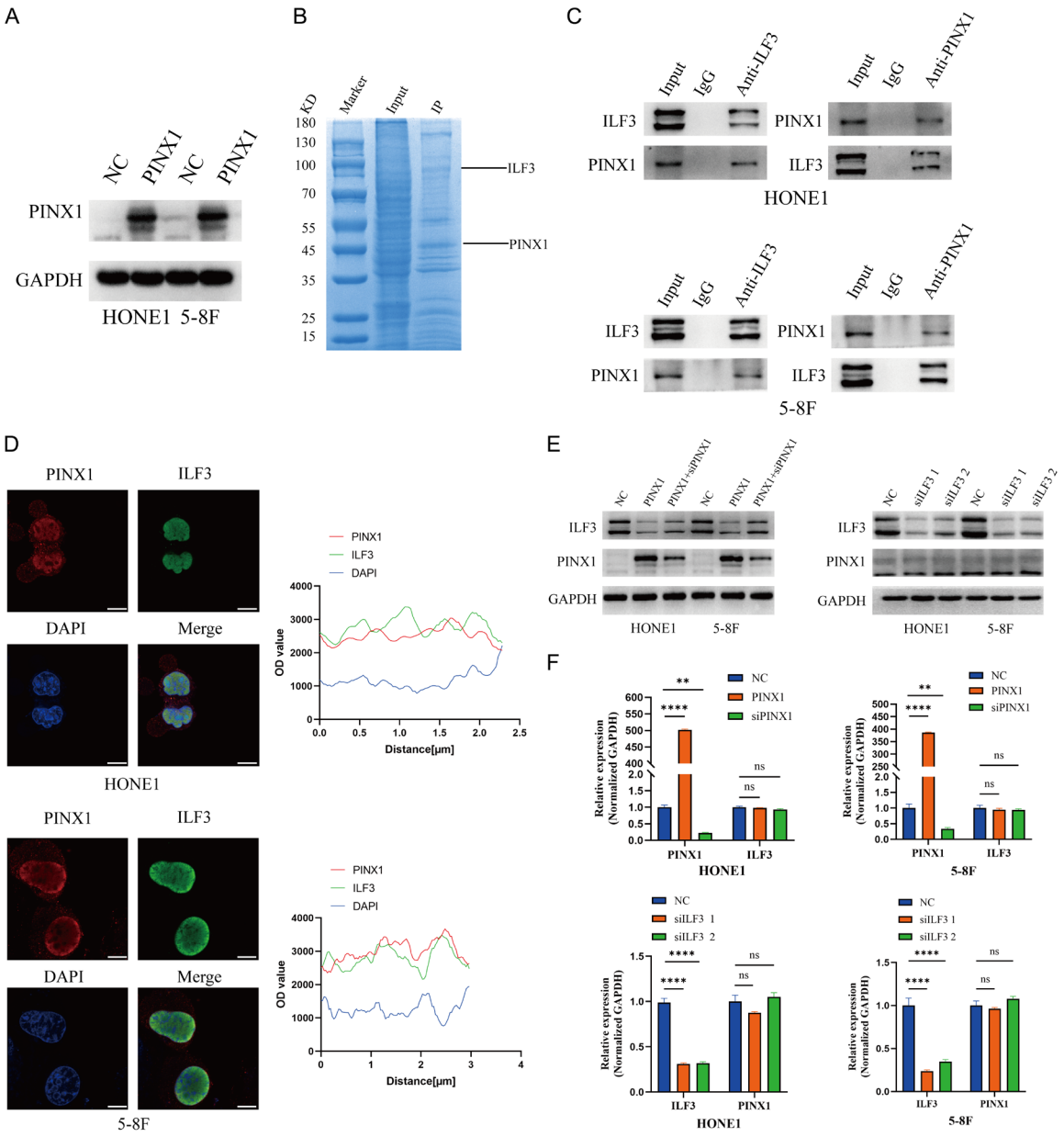

Figure 3. PINX1 promotes ILF3 ubiquitination via SPOP. PINX1 Promotes ILF3 Ubiquitination via SPOP. A. PINX1 overexpression in Hone1 and 5-8F cells was detected by Western blotting; B. Coomassie brilliant blue staining showed the proteins that interacted with PINX1 in 5-8F cells and the molecular weights of PINX1 and ILF3; C. Co-immunoprecipitation (Co-IP) verifies the combination of PINX1 and ILF3; D. The co-localization of PINX1 and ILF3 proteins was detected by immunofluorescence (×1000, Scale bar: 10 μm); E. The changes of PINX1 and ILF3 protein expression after overexpression and knockdown were detected by Western blotting; F. The changes of PINX1 and ILF3 mRNA expression after overexpression and knockdown were detected by Western blotting. ILF3: Interleukin enhancer-binding factor 3; siILF3: ILF3 knockdown; PINX1: PIN2/TRF1-interacting telomerase inhibitor 1; NPC: Nasopharyngeal carcinoma; NP: Nasopharyngeal; HONE1 and 5-8F: Human Nasopharyngeal Epithelial cell line (HONE1 and 5-8F); SPOP: Speckle-type BTB/POZ protein; *, *P*<0.05; **, *P*<0.01; ***, *P*<0.001; ****, *P*<0.0001.

Overexpression of PINX1 reduced ILF3 protein levels, but ILF3 had no effect on PINX1 levels (**Figure 3E**). qPCR showed that neither PINX1 nor ILF3 mRNA levels changed significantly following overexpression or knockdown of the other gene (both P>0.05), indicating a post-transcriptional regulatory mechanism (**Figure 3F**).

PINX1 recruits E3 ubiquitin ligase SPOP to regulate ILF3 stability

To investigate the mechanism underlying PINX1-mediated regulation of ILF3, we examined its interaction with the E3 ubiquitin ligase SPOP. Co-IP assays demonstrated that PINX1 recruited SPOP to form a ubiquitin ligase complex (**Figure 4A**, **4B**). Immunofluorescence confirmed this co-localization (**Figure 4C**).

CHX chase assays showed that PINX1 overexpression accelerated ILF3 protein degradation, while MG132 treatment blocked this effect (**Figure 4D**). Ubiquitination assays confirmed that PINX1 increased ILF3 ubiquitination in both HONE1 and 5-8F cells. Notably, SPOP knockdown abolished the effect of PINX1 on ILF3 protein levels, and Co-IP results demonstrated that SPOP depletion attenuated PINX1-mediated ILF3 ubiquitination and degradation (**Figure 4E**).

STAT3 suppresses PINX1 transcription

To determine whether STAT3 regulates PINX1 expression, we modulated STAT3 levels in NPC cells. Knockdown of STAT3 using siRNA led to increased PINX1 expression at both protein and mRNA levels (**Figure 5A**, **5B**), while STAT3 overexpression decreased PINX1 expression (**Figure 5C**). Treatment with Stattic, a STAT3 inhibitor, induced a dose-dependent upregulation of PINX1 (**Figure 5D**).

ChIP assays showed that STAT3 bound to the PINX1 promoter at site 1 (-1356 to -1346) and site 2 (-1327 to -1317), but not at site 3 (-1139 to -1129) (**Figure 5E**). Electrophoretic mobility shift assays confirmed STAT3 binding to the PINX1 promoter (**Figure 5F**). Dual-luciferase reporter assays further validated that STAT3 suppressed PINX1 promoter activity, and mutation of the STAT3-binding sites partially restored transcriptional activity (**Figure 5G**).

PINX1 reversed ILF3-induced proliferation and chemoresistance in vitro

CCK-8 and cell cycle assays demonstrated that PINX1 overexpression significantly counteracted ILF3-induced increases in cell viability in HONE1 and 5-8F cells (**Figure 6A**, **6B**). EdU assays similarly confirmed that PINX1 overexpression reversed ILF3-driven proliferation (**Figure 6C**). Moreover, PINX1 overexpression also reversed ILF3-induced proliferation and cisplatin (DDP) resistance in both cell lines (**Figure 6D**, **6E**).

PINX1 knockdown promotes tumor progression in vivo and enhances chemotherapy sensitivity

In vivo, xenografts generated using PINX1-knockdown 5-8F cells displayed increased tumor volume and weight compared to controls (shNC group) (**Figure 7A-C**). Immunohistochemical staining showed elevated levels of Ki-67 and PCNA in tumors from the PINX1-knockdown group. In contrast, DDP- and Stattic-treated tumors exhibited the lowest expression of these proliferation markers (**Figure 7D**). The strongest suppression of Ki-67 and PCNA was observed in the combination group receiving full-dose DDP and Stattic, supporting the role of PINX1 in reducing both tumor proliferation and DDP resistance.

Discussion

This study systematically elucidates the functional roles and regulatory mechanisms of ILF3 and PINX1 in NPC development. We report for the first time that ILF3 and PINX1 interact functionally in NPC, forming a STAT3-PINX1-ILF3 axis that regulates the PI3K-AKT-mTOR signaling pathway. This regulatory cascade affects tumor proliferation, chemoresistance, and clinical prognosis, providing a novel theoretical foundation for NPC-targeted therapies.

Telomerase activation is essential for the immortalization, malignant transformation, and progression of nasopharyngeal epithelial cells [19]. Human telomerase reverse transcriptase (hTERT), the catalytic subunit of telomerase, is frequently upregulated in NPC and supports both uncontrolled proliferation and therapeutic resistance [20]. Targeting regulators of telomerase activity is therefore a promising thera-

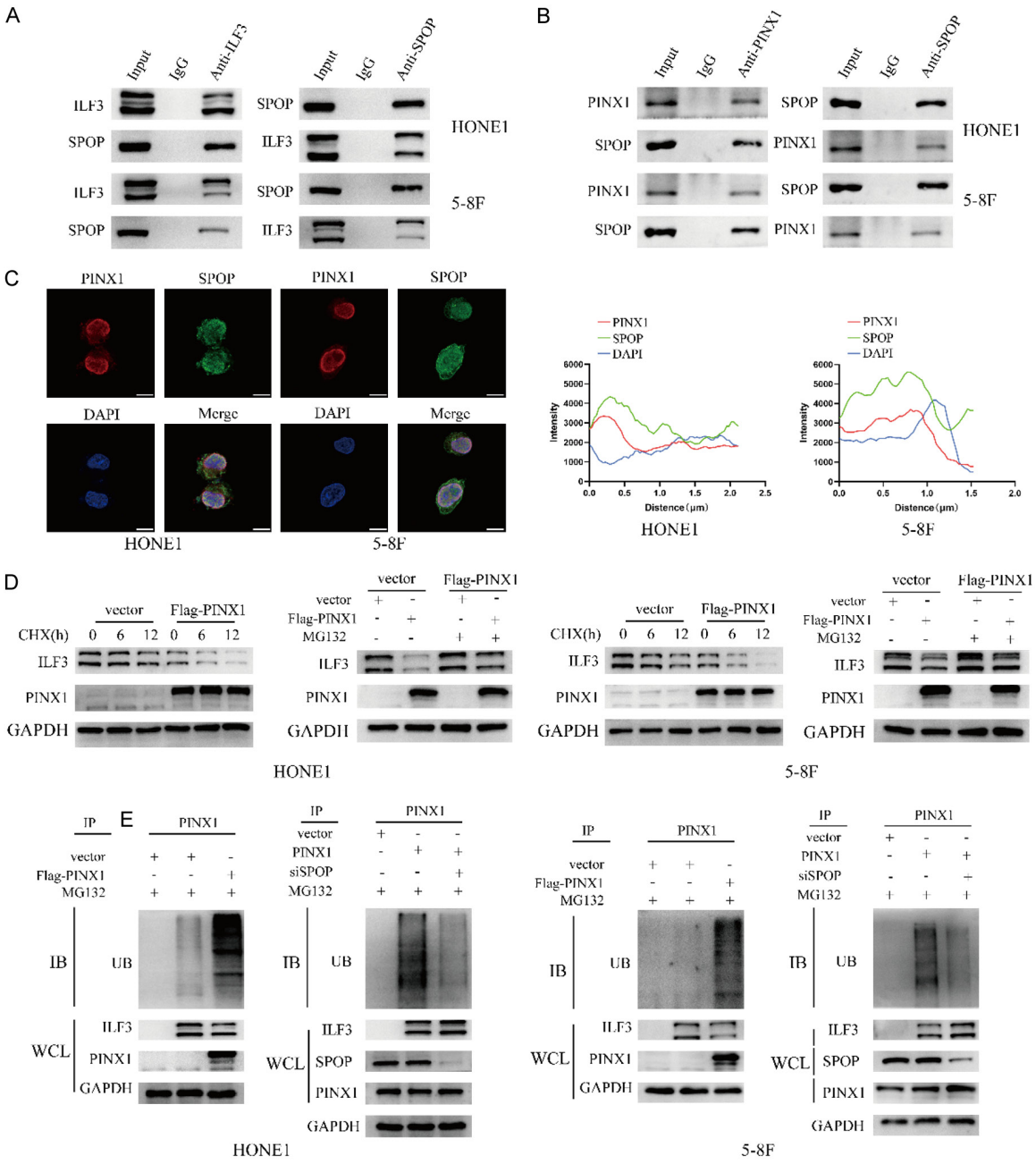

Figure 4. PINX1 recruits E3 ubiquitin ligase SPOP to regulate ILF3 protein stability. PINX1 recruits E3 ubiquitin ligase SPOP to regulate ILF3 protein stability. A, B. Co-IP detected the interaction of PINX1, ILF3, and SPOP; C. The co-localization of PINX1, ILF3 and SPOP was detected by immunofluorescence (×1000, Scale bar: 10 μm); D, E. Cycloheximide (CHX) chase, MG-132 and ubiquitination assays show that PINX1 promotes ILF3 degradation via SPOP and can reverse the degradation upon SPOP knockdown. ILF3: Interleukin enhancer-binding factor 3; siILF3: ILF3 knockdown; PINX1: PIN2/TRF1-interacting telomerase inhibitor 1; NPC: Nasopharyngeal carcinoma; NP: Nasopharyngeal; HONE1 and 5-8F: Human Nasopharyngeal Epithelial cell line; SPOP: Speckle-type BTB/POZ protein; *, $P<0.05$; **, $P<0.01$; ***, $P<0.001$; ****, $P<0.0001$.

peutic approach. PINX1 is a well-characterized tumor suppressor that inhibits telomerase through direct binding to hTERT, thereby suppressing its catalytic activity [16]. Recent evidence has shown that PINX1 also exerts tumor-suppressive effects independent of telomerase inhibition, including roles in DNA damage repair, cell cycle control, and protein degradation path-

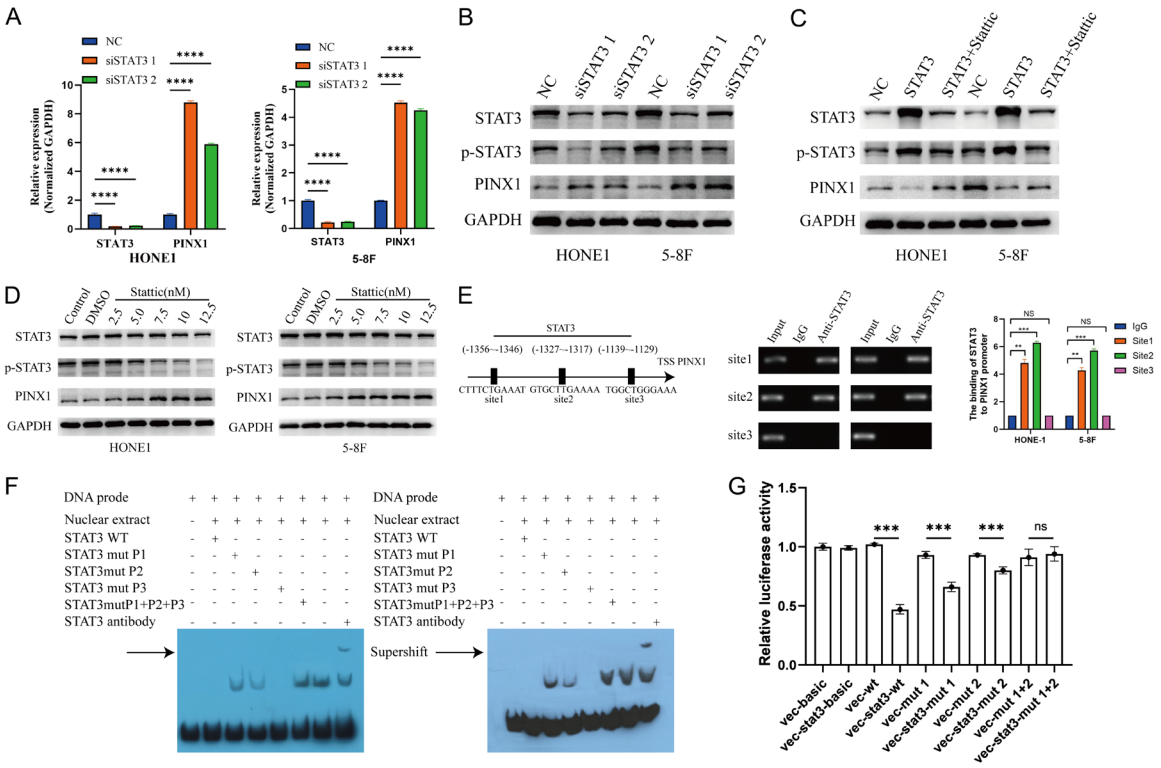

Figure 5. STAT3 suppresses PINX1 expression through transcriptional regulation. STAT3 suppresses PINX1 expression through transcriptional regulation. A. qPCR experiments of PINX1 expression upon STAT3 knockdown; B, C. Western blotting experiments of PINX1 expression upon STAT3 knockdown, inhibition, and overexpression; D. The levels of PINX1 following treatment with Static, a STAT3 inhibitor; E. ChIP assays were conducted to verify the presence of STAT3 binding sites in the PINX1 promoter; F. EMSA assay confirmed the binding of STAT3 to the promoter of PINX1; G. Luciferase Activity Report confirmed that STAT3 represses PINX1 transcription. ILF3: Interleukin enhancer-binding factor 3; siILF3: ILF3 knockdown; PINX1: PIN2/TRF1-interacting telomerase inhibitor 1; NPC: Nasopharyngeal carcinoma; NP: Nasopharyngeal; HONE1 and 5-8F: Human Nasopharyngeal Epithelial cell line; *, P<0.05; **, P<0.01; ***, P<0.001; ****, P<0.0001.

ways [19]. Notably, studies have revealed that PINX1 expression is significantly reduced in NPC tissues, independent of genetic mutations or promoter methylation [20]. However, the mechanisms responsible for this downregulation remain poorly understood.

PINX1 does not function as a kinase, phosphatase, or transcription factor but instead exerts its effects primarily through protein-protein interactions [14]. In our study, ILF3 was found to be significantly upregulated, and PINX1 significantly downregulated, in NPC cell lines compared to NP69. This expression pattern was consistent with immunohistochemical findings in patient samples. ILF3 and PINX1 expression correlated with clinical stage, TNM stage. Prognostically, patients with low PINX1 and high ILF3 expression had the poorest outcomes. Multivariate Cox regression analysis further identified ILF3 and PINX1 expression, along with clinical stage and TNM classification, as independent predictors of patient prognosis. These findings align with those of Yang et al. [21], who reported that elevated ILF3 expression was associated with advanced disease stage and poor survival. Similarly, low PINX1 expression has been implicated in poor outcomes across multiple cancer types [13].

GSEA and functional assays confirmed that ILF3 promotes cell proliferation and DDP resistance by activating the PI3K-AKT-mTOR pathway. ILF3 overexpression significantly increased phosphorylation levels of PI3K, AKT, and mTOR, as well as expression of the cell cycle regulator CCNE1. These results are consistent with those of Yan et al. [22], who reported that ILF3 mediates mTORC1-dependent amino acid-induced signaling. Moreover, ILF3 knockdown reduced the IC_{50} of DDP by nearly 50%, suggesting that ILF3 inhibition may improve chemotherapeutic efficacy in NPC.

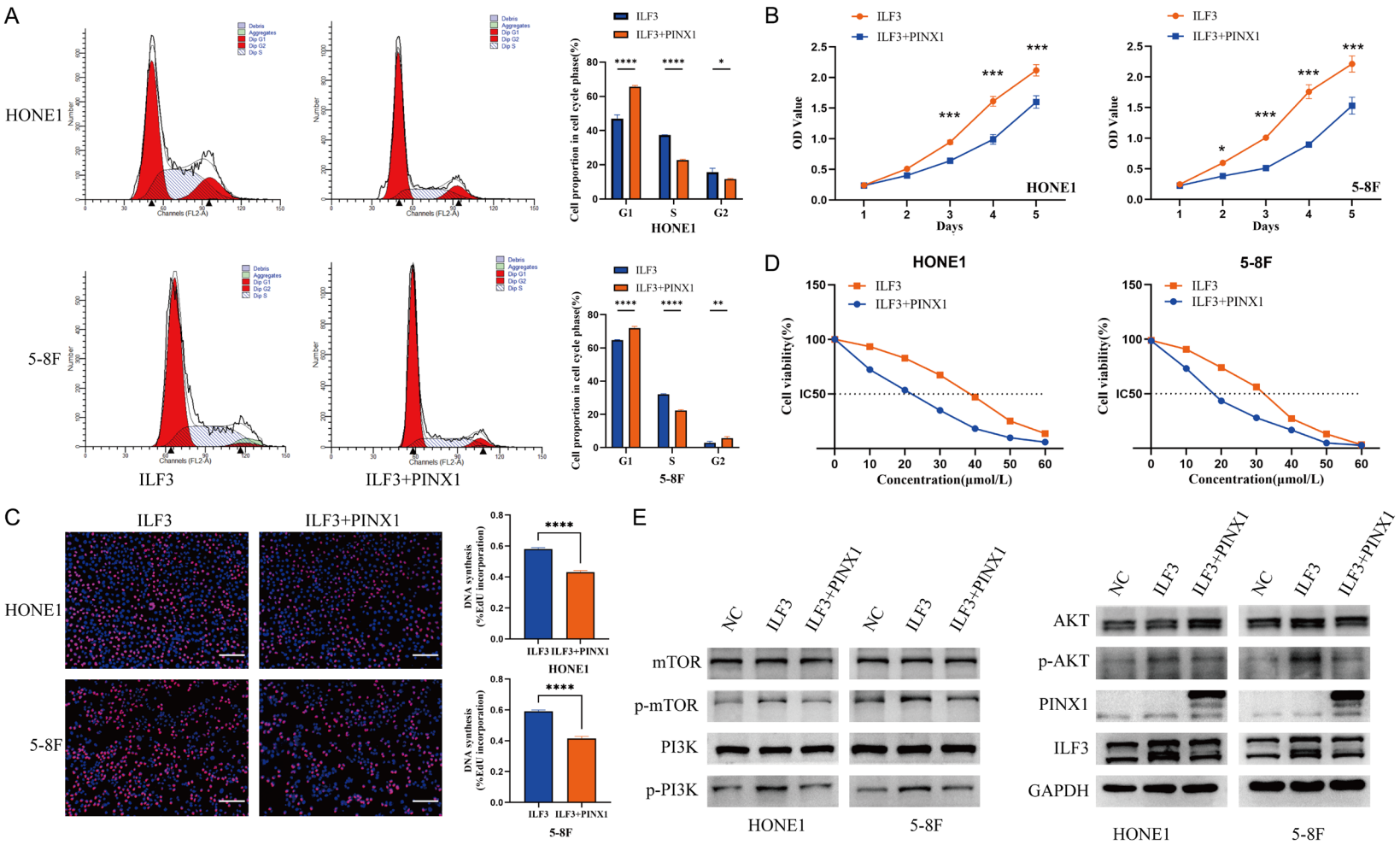

Figure 6. PINX1 reversed ILF3-induced proliferation and chemotherapy resistance in vitro. Note: (A) Cell cycle assay of PINX1 overexpression on ILF3-induced HONE1 and 5-8F cells viability; (B) CCK-8 detection of PINX1 overexpression on ILF3-induced HONE1 and 5-8F cells viability; (C) EdU detection of PINX1 overexpression on ILF3-induced HONE1 and 5-8F cells proliferation (×100, Scale bar: 200 μm); (D, E) CCK-8 and Western blotting detection of PINX1 overexpression on ILF3-induced HONE1 and 5-8F cells proliferation and DDP resistance. ILF3: Interleukin enhancer-binding factor 3; PINX1: PIN2/TRF1-interacting telomerase inhibitor 1; NPC: Nasopharyngeal carcinoma; NP: Nasopharyngeal; HONE1 and 5-8F: Human Nasopharyngeal Epithelial cell line; *, P<0.05; **, P<0.01; ***, P<0.001; ****, P<0.0001.

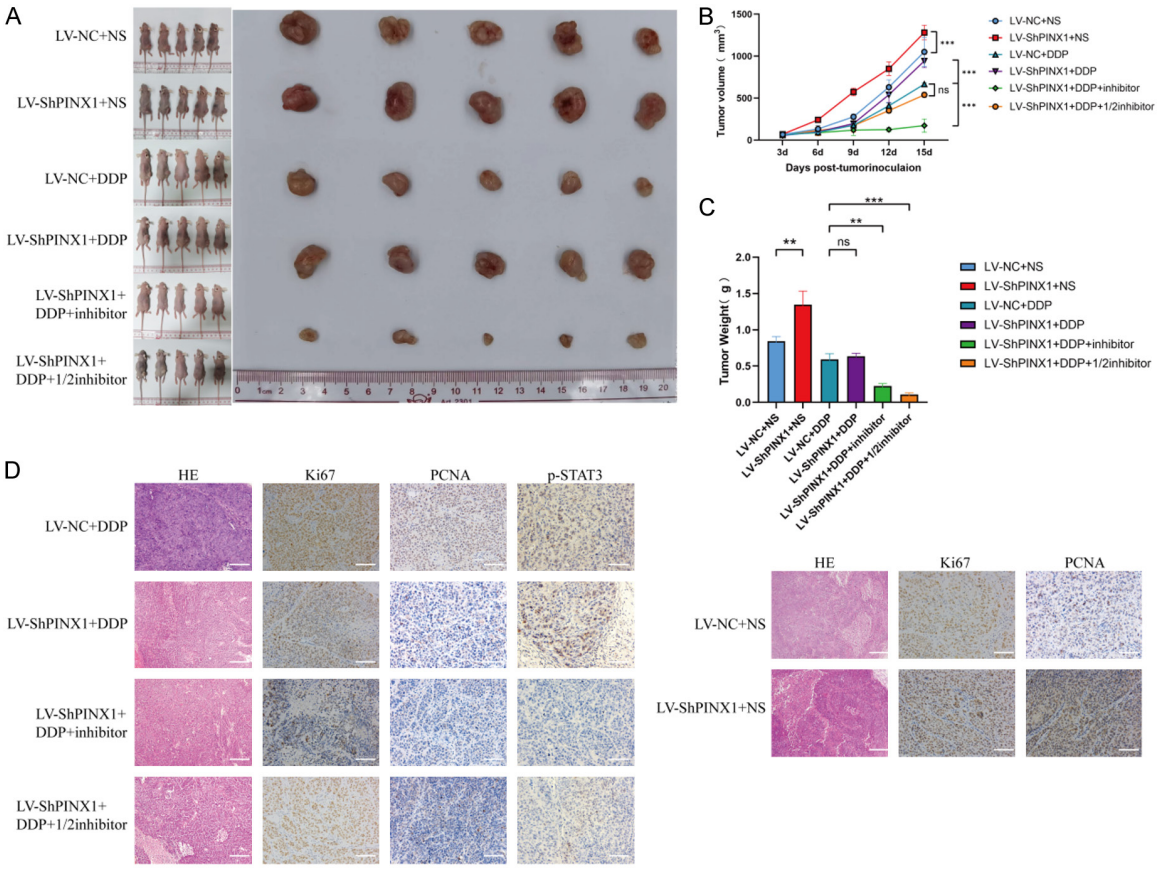

Figure 7. PINX1 knockdown promoted tumor progression in vivo and enhances chemotherapy sensitivity. Note: (A) PINX1 knockdown and drug therapy and tumor size change in nude mice; (B) PINX1 knockdown and drug therapy and tumor volume change in nude mice; (C) PINX1 knockdown and drug therapy and body weight change in nude mice; (D) Detection of Ki-67, PCNA, and p-STAT3 with immunohistochemical staining in tumor tissues (×200, Scale bar: 100 μm). PINX1: PIN2/TRF1-interacting telomerase inhibitor 1; NPC: Nasopharyngeal carcinoma; NP: Nasopharyngeal; HONE1 and 5-8F: Human Nasopharyngeal Epithelial cell line; *, P<0.05; **, P<0.01; ***, P<0.001; ****, P<0.0001.

Mass spectrometry and Co-IP assays confirmed that PINX1 directly interacts with ILF3. Mechanistically, PINX1 promotes ILF3 degradation by recruiting the E3 ubiquitin ligase SPOP. While PINX1 did not affect ILF3 mRNA levels, it significantly reduced ILF3 protein levels, indicating a post-translational mode of regulation. Follow-up biochemical analyses demonstrated that PINX1 overexpression reduced ILF3 protein stability, shortened its half-life, and markedly increased ILF3 ubiquitination, leading to proteasomal degradation [23]. Thus, PINX1 functions as a scaffold protein that facilitates SPOP-mediated ubiquitination of ILF3 [24].

Taken together, these findings position PINX1 as a dual-function tumor suppressor in NPC - negatively regulating ILF3 protein stability and antagonizing PI3K-AKT-mTOR-driven oncogenic signaling.

Our study demonstrates that STAT3 negatively regulates PINX1 expression, significantly reinforcing the existence of a STAT3-PINX1-ILF3 signaling axis in NPC progression. STAT3 is a well-established oncogenic transcription factor that promotes cell survival, proliferation, and immune evasion through transcriptional activation of target genes [25]. EBV, a key oncogenic driver in NPC, has been shown to activate STAT3 signaling and enhance tumor progression [26]. In our experiments, STAT3 overexpression suppressed PINX1 expression, while STAT3 inhibition - either via siRNA or the pharmacological inhibitor Stattic - increased PINX1 expression. Bioinformatic analysis identified

three putative STAT3-binding sites in the PINX1 promoter, which were validated by ChIP-qPCR and dual-luciferase reporter assays.

These findings provide novel mechanistic insights into the PINX1-ILF3-PI3K-AKT-mTOR regulatory axis in NPC and highlight PINX1 as a promising therapeutic target. Since ILF3 promotes tumor progression and chemoresistance, its degradation - mediated by PINX1 - may represent a viable therapeutic strategy. Moreover, the transcriptional repression of PINX1 by STAT3 suggests that combining a STAT3 inhibitor (e.g., Stattic) with standard chemotherapy (e.g., cisplatin) may enhance treatment efficacy [20]. Supporting this, our in vivo experiments showed that the combination of Stattic and DDP produced the most pronounced tumor-suppressive effects in NPC xenograft models, resulting in significant reductions in tumor burden and proliferation markers (Ki-67 and PCNA).

Given the frequent activation of STAT3 in EBV-associated NPC, targeting the STAT3-PINX1-ILF3 axis may offer a clinically relevant strategy for managing advanced or chemoresistant NPC.

While our study provides important mechanistic insights into the role of PINX1 in NPC, several limitations should be noted. First, the findings are primarily based on in vitro analyses and xenograft models, as well as a single-center cohort of 99 NPC patients, necessitating validation in larger, multi-center studies. Second, while Stattic is a widely used inhibitor of STAT3 phosphorylation and activity, its potential off-target effects remain a concern. Future studies should explore the use of more selective STAT3 inhibitors or gene-editing approaches (e.g., CRISPR-Cas9) to more precisely disrupt STAT3 function in NPC. Third, although we demonstrate that PINX1 directly interacts with ILF3, the broader regulatory network of PINX1 remains poorly understood. Additional research is needed to investigate whether PINX1 also interacts with other oncogenic pathways or protein partners. Finally, functional differences in PINX1 activity between EBV-positive and EBV-negative NPC subtypes remain unclear and warrant further investigation.

Addressing these limitations will be critical to advancing PINX1 as a clinically relevant therapeutic target in NPC.

In conclusion, we identify PINX1 as a tumor suppressor in NPC that negatively regulates ILF3 protein stability via SPOP-mediated ubiquitination. ILF3 promotes tumor progression and chemoresistance through activation of the PI3K-AKT-mTOR signaling pathway, and stabilization of PINX1 can counteract these oncogenic effects. Transcriptionally, PINX1 is suppressed by STAT3, suggesting the presence of a novel STAT3-PINX1-ILF3 regulatory axis in NPC. Targeting STAT3 with inhibitors such as Stattic, in combination with chemotherapeutic agents like cisplatin, may enhance treatment efficacy in NPC.

This study offers new mechanistic insights and proposes a potential therapeutic strategy for NPC, positioning PINX1 as both a biomarker and druggable target. Future investigations should validate the clinical utility of STAT3 inhibitors in NPC, elucidate the specific mechanisms underlying their antitumor effects, and further explore the PINX1 interaction network beyond ILF3.

Acknowledgements

The authors thank the Central Laboratory of Integrated Hospital of Traditional Chinese Medicine of the Southern Medical University of Guangdong Province for assisting with the experiment. This work was supported by the National Natural Science Foundation of China [grant number 81572666]; the Science and Technology Program Foundation of Guangzhou [grant number 20170710382]; and The Young Investigator grants of Guangdong Provincial Second People's Hospital [grant number YQ2017-007].

Disclosure of conflict of interest

None.

Abbreviations

PINX1, PIN2/TERF1-interacting telomerase inhibitor 1; ILF3, interleukin-enhancer binding factor 3; NPC, nasopharyngeal carcinoma; DDP, cisplatin; ChIP, chromatin immunoprecipitation; Co-IP, co-Immunoprecipitation; CHX, cycloheximid; EMSA, electrophoretic mobility shift assay.

Address correspondence to: Hong Peng, Department of Otolaryngology-Head and Neck Surgery, Guangdong Second Provincial General Hospital, No.

466 Xingang Middle Road, Haizhu District, Guangzhou 510220, Guangdong, China. E-mail: doctorpenghong@163.com

References

[1] Clark PE, Taparra K and Miller JA. Identification of high-incidence populations in the united states for anti-epstein-barr virus serologic screening for nasopharyngeal carcinoma. Cancer Epidemiol Biomarkers Prev 2024; 33: 1706-1716.

[2] Smith C. EBV and nasopharyngeal carcinoma: a target for cellular therapies. Immunotherapy 2013; 5: 821-824.

[3] Huang D, Song SJ, Wu ZZ, Wu W, Cui XY, Chen JN, Zeng MS and Su SC. Epstein-Barr virus-induced VEGF and GM-CSF drive nasopharyngeal carcinoma metastasis via recruitment and activation of macrophages. Cancer Res 2017; 77: 3591-3604.

[4] Liu H, Tang L, Li Y, Xie W, Zhang L, Tang H, Xiao T, Yang H, Gu W, Wang H and Chen P. Nasopharyngeal carcinoma: current views on the tumor microenvironment's impact on drug resistance and clinical outcomes. Mol Cancer 2024; 23: 20.

[5] Chen S, Luo Y, Ruan S, Su G and Huang G. RNA binding protein ILF3 increases CEP55 mRNA stability to enhance malignant potential of breast cancer cells and suppress ferroptosis. Hereditas 2025; 162: 10.

[6] Xu Z, Huang H, Li X, Ji C, Liu Y, Liu X, Zhu J, Wang Z, Zhang H and Shi J. High expression of interleukin-enhancer binding factor 3 predicts poor prognosis in patients with lung adenocarcinoma. Oncol Lett 2020; 19: 2141-2152.

[7] Shen HM, Zhang D, Xiao P, Qu B and Sun YF. E2F1-mediated KDM4A-AS1 up-regulation promotes EMT of hepatocellular carcinoma cells by recruiting ILF3 to stabilize AURKA mRNA. Cancer Gene Ther 2023; 30: 1007-1017.

[8] Zhang Y, Wang K, Yang D, Liu F, Xu X, Feng Y, Wang Y, Zhu S, Gu C, Sheng J, Hu L, Xu B, Lu YJ and Feng N. Hsa_circ_0094606 promotes malignant progression of prostate cancer by inducing M2 polarization of macrophages through PRMT1-mediated arginine methylation of ILF3. Carcinogenesis 2023; 44: 15-28.

[9] Sur S, Nakanishi H, Steele R, Zhang D, Varvares MA and Ray RB. Long non-coding RNA ELDR enhances oral cancer growth by promoting ILF3-cyclin E1 signaling. EMBO Rep 2020; 21: e51042.

[10] Li P, Mi Q, Yan S, Xie Y, Cui Z, Zhang S, Wang Y, Gao H, Wang Y, Li J, Du L and Wang C. Characterization of circSCL38A1 as a novel oncogene in bladder cancer via targeting ILF3/TGF-β2 signaling axis. Cell Death Dis 2023; 14: 59.

[11] Hu Y, Cai ZR, Huang RZ, Wang DS, Ju HQ and Chen DL. Circular RNA circPHLPP2 promotes tumor growth and anti-PD-1 resistance through binding ILF3 to regulate IL36γ transcription in colorectal cancer. Mol Cancer 2024; 23: 272.

[12] Weng Y, Yan X, Chen B, Bian Z, Ge Y, Lu H, He S, Wu J, Chen Y, Lei M and Zhang Y. PinX1 suppresses cancer progression by inhibiting telomerase activity in cervical squamous cell carcinoma and endocervical adenocarcinoma. Genes Dis 2024; 12: 101319.

[13] Huang M, Zhu X, Wang C, He L, Li L, Wang H, Fan G and Wang Y. PINX1 loss confers susceptibility to PARP inhibition in pan-cancer cells. Cell Death Dis 2024; 15: 610.

[14] Qiu J, Xia Y, Bao Y, Cheng J, Liu L and Qian D. Silencing PinX1 enhances radiosensitivity and antitumor-immunity of radiotherapy in non-small cell lung cancer. J Transl Med 2024; 22: 228.

[15] Kang J, Park JH, Kong JS, Kim MJ, Lee SS, Park S and Myung JK. PINX1 promotes malignant transformation of thyroid cancer through the activation of the AKT/MAPK/β-catenin signaling pathway. Am J Cancer Res 2021; 11: 5485-5495.

[16] You D, Tong K, Li Y, Zhang T, Wu Y, Wang L, Chen G and Zhang X. PinX1 plays multifaceted roles in human cancers: a review and perspectives. Mol Biol Rep 2024; 51: 1163.

[17] Liu Y, Gong P, Zhou N, Zhang J, He C, Wang S and Peng H. Insufficient PINX1 expression stimulates telomerase activation by direct inhibition of EBV LMP1-NF-κB axis during nasopharyngeal carcinoma development. Biochem Biophys Res Commun 2019; 514: 127-133.

[18] Guo C, Luo J, Liang M and Xiao J. Correlation of 18 F-FDG PET/CT metabolic parameters with Ki-67 expression and tumor staging in nasopharyngeal carcinoma. Nucl Med Commun 2025; 46: 437-443.

[19] Liu M, Zhang Y, Jian Y, Gu L, Zhang D, Zhou H, Wang Y and Xu ZX. The regulations of telomerase reverse transcriptase (TERT) in cancer. Cell Death Dis 2024; 15: 90.

[20] Xiang H, Liu L, Yuan Y, Liu L and Chen Z. Inhibition mechanism of PinX1 gene on cancer stem cells of nasopharyngeal carcinoma. Cell Mol Biol (Noisy-le-grand) 2022; 68: 182-186.

[21] Yang X, Lin F and Gao F. Up-regulated long noncoding RNA ILF3-AS1 indicates poor prognosis of nasopharyngeal carcinoma and promoted cell metastasis. Int J Biol Markers 2020; 35: 61-70.

[22] Yan G, Yang J, Li W, Guo A, Guan J and Liu Y. Genome-wide CRISPR screens identify ILF3 as a mediator of mTORC1-dependent amino acid sensing. Nat Cell Biol 2023; 25: 754-764.

[23] Lian Q, Gao Y, Li Q, He X, Jiang X, Pu Z and Xu G. Cereblon promotes the ubiquitination and

proteasomal degradation of interleukin enhancer-binding factor 2. Protein J 2020; 39: 411-421.
[24] Li HL, Song J, Yong HM, Hou PF, Chen YS, Song WB, Bai J and Zheng JN. PinX1: structure, regulation and its functions in cancer. Oncotarget 2016; 7: 66267-66275.
[25] Tošić I and Frank DA. STAT3 as a mediator of oncogenic cellular metabolism: pathogenic and therapeutic implications. Neoplasia 2021; 23: 1167-1178.
[26] Ren Y, Yang J, Li M, Huang N, Chen Y, Wu X, Wang X, Qiu S, Wang H and Li X. Viral IL-10 promotes cell proliferation and cell cycle progression via JAK2/STAT3 signaling pathway in nasopharyngeal carcinoma cells. Biotechnol Appl Biochem 2020; 67: 929-938.